Acta Crystallographica Section F
Structural Biology and Crystallization Communications
ISSN 1744-3091

Structure of autophagy-related protein Atg8 from the silkworm *Bombyx mori*

Chen Hu, Xuan Zhang, Yan-Bin Teng, Hai-Xi Hu and Wei-Fang Li*

Hefei National Laboratory for Physical Sciences at Microscale and School of Life Sciences, University of Science and Technology of China, People's Republic of China

Correspondence e-mail: liwf@ustc.edu.cn

Received 19 April 2010
Accepted 18 May 2010

PDB Reference: autophagy-related protein Atg8, 3m95.

Autophagy-related protein Atg8 is ubiquitous in all eukaryotes. It is involved in the Atg8–PE ubiquitin-like conjugation system, which is essential for autophagosome formation. The structures of Atg8 from different species are very similar and share a ubiquitin-fold domain at the C-terminus. In the 2.40 Å crystal structure of Atg8 from the silkworm *Bombyx mori* reported here, the ubiquitin fold at the C-terminus is preceded by two additional helices at the N-terminus.

1. Introduction

Autophagy is essential for cell survival in all eukaryotes and is involved in the degradation of cytoplasmic components and intracellular proteins by lysosomes (Reggiori & Klionsky, 2002). Cell signals such as starvation can stimulate autophagy and induce the formation of a double-membrane structure called the autophagosome, which docks and fuses with the lysosome, whereupon the inner contents of the autophagosome are released into the lysosome and are consumed by hydrolases (Shintani & Klionsky, 2004; Reggiori & Klionsky, 2002). Recent studies have revealed a wide variety of physiological roles of autophagy and its relevance to diseases such as liver diseases, muscular disorders, neurodegeneration, pathogen infections and cancer (Cuervo, 2004).

Several autophagy-related genes (*ATG*s) have been identified in *Saccharomyces cerevisiae*. Two ubiquitin-like conjugation systems (the Atg8–PE system and the Atg12–Atg5–Atg16 system) are essential for autophagosome formation (Klionsky *et al.*, 2003; Amar *et al.*, 2006). In the Atg8–PE system, the removal of the carboxyl-terminal arginine from newly synthesized Atg8 by a cysteine protease, Atg4, exposes a glycine residue at the carboxyl-terminus. The uncovered glycine is then activated and covalently conjugated to phosphatidylethanolamine (PE) by the E1-like enzyme Atg7 and the E2-like enzyme Atg3 (Ichimura *et al.*, 2000). The Atg8–PE system controls the expansion of the autophagosome precursor, the phagophore (Xie *et al.*, 2008), and directly determines the growth of autophagosomal membranes (Nakatogawa *et al.*, 2007).

Recently, several autophagy-related genes have been identified in *Bombyx mori* (Zhang *et al.*, 2009). *BmATG8* (Genbank accession No. FJ416330), which encodes a homologue of yeast Atg8, was found to be up-regulated in the silk gland in fifth-instar *B. mori* larvae, suggesting that BmAtg8 may play an important role in maturation of the silk gland (Zhang *et al.*, 2009).

Here, we report the crystal structure of BmAtg8 at 2.40 Å resolution. BmAtg8 consists of the ubiquitin fold at the C-terminus, which is conserved among species from yeast to mammals, with two additional helices at the N-terminus.

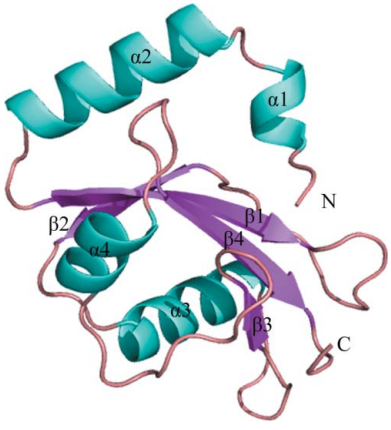

2. Materials and methods

2.1. Cloning and protein expression

The gene encoding residues 1–116 of BmAtg8 was amplified by PCR from the total RNA of *B. mori*. The amplified DNA was cloned

into pET28a-derived vector plasmid using primers with *Nde*I and *Not*I restriction sites. The resulting construct was verified by sequencing and contained an MHHHHHHG tag at the N-terminus of the protein. *Escherichia coli* BL21 (DE3) cells were transformed with this construct and were cultured in 400 ml 2×YT medium containing 10 µg ml^{-1} kanamycin at 310 K until the OD_{600} reached 0.6. Protein expression was induced using isopropyl β-D-1-thiogalactopyranoside at a final concentration of 0.2 m*M* at 310 K for 4 h. Cells were harvested by centrifugation at 7330*g* for 10 min and resuspended in lysis buffer (20 m*M* Tris–HCl pH 8.5, 50 m*M* NaCl). The suspension was sonicated and the supernatant was collected by centrifugation at 12 000*g* for 30 min at 277 K.

2.2. Purification

The supernatant was loaded onto 2 ml Ni–NTA affinity resin (GE Healthcare Bioscience) with lysis buffer at 289 K. After washing with 20 ml 10 m*M* imidazole in lysis buffer, the target protein of about 14 kDa was eluted with lysis buffer containing 250 m*M* imidazole and was then further purified on a HiLoad Superdex 75 column (GE Healthcare Bioscience) equilibrated with lysis buffer at 289 K. The fractions containing the target protein were verified using 15% SDS–PAGE.

2.3. Crystallization and data collection

Purified protein solution (in 20 m*M* Tris–HCl pH 8.5, 50 m*M* NaCl) was concentrated to 20 mg ml^{-1} by ultrafiltration (Millipore Amicon) into lysis buffer with a final concentration of 4 m*M* dithiothreitol (DTT). Crystallization conditions were screened by the sitting-drop vapour-diffusion method at 291 K using Crystal Screens I and II and Index I and II (Hampton Research). Crystals obtained in a condition consisting of 2.0 *M* ammonium sulfate, 0.1 *M* sodium citrate pH 5.6 and 0.2 *M* sodium/potassium tartrate were reproduced and grown to a useful size by the hanging-drop vapour-diffusion method. The drops consisted of 1 µl protein solution and 1 µl reservoir solution and were equilibrated against 500 µl reservoir solution. The crystal used for data collection was flash-frozen in liquid nitrogen using a cryoprotectant consisting of the reservoir solution plus 25%(*v*/*v*) glycerol. Diffraction data were collected to 2.40 Å resolution at 100 K using an in-house Rigaku MM007 X-ray generator (λ = 1.5418 Å) with a MAR Research 345 dtb detector (MAR Research, Germany) at the School of Life Sciences, University of Science and Technology of China (USTC; Hefei, People's Republic of China).

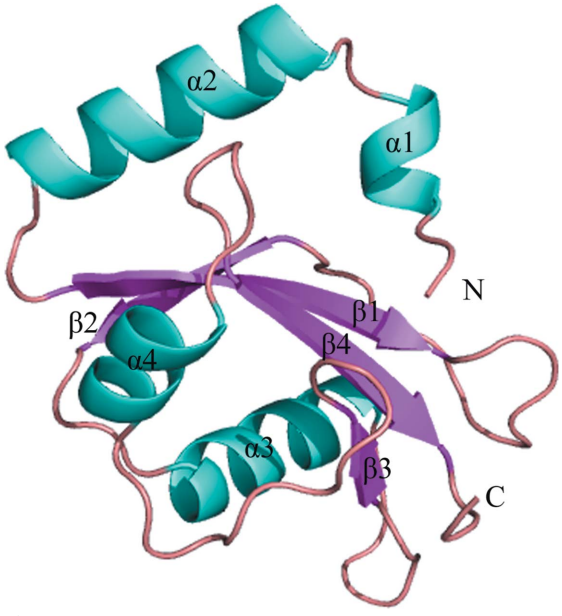

Figure 1
The overall structure of BmAtg8. α-Helices are coloured cyan and β-strands are coloured magenta. This figure was prepared using *PyMOL* (DeLano, 2002).

Table 1
Crystal parameters, data-collection and structure-refinement statistics.

Values in parentheses are for the highest resolution bin.

Data processing	
Resolution range (Å)	27.08–2.40 (2.46–2.40)
Space group	$P4_1$
Unit-cell parameters (Å, °)	$a = b = 96.77$, $c = 44.31$, $\alpha = \beta = \gamma = 90.00$
Unique reflections	14385 (765)
Completeness (%)	92.7 (90.2)
Mean $I/\sigma(I)$	14.4 (1.7)
R_{merge}† (%)	8.3 (32.9)
Refinement statistics	
Resolution range (Å)	27.08–2.40
R factor‡/R_{free}§ (%)	23.11/27.31
Mean B factor (Å^2)	48.69
No. of protein atoms	1949
No. of water atoms	69
R.m.s.d.¶ bond lengths (Å)	0.015
R.m.s.d.¶ bond angles (°)	1.448
Ramachandran plot††	
Residues in most favoured regions (%)	95.15
Residues in additional allowed regions (%)	4.85
Residues in disallowed regions (%)	0

† $R_{merge} = \sum_{hkl}\sum_i |I_i(hkl) - \langle I(hkl)\rangle| / \sum_{hkl}\sum_i I_i(hkl)$, where $I_i(hkl)$ is the intensity of an observation and $\langle I(hkl)\rangle$ is the mean value for its unique reflection; summations are over all reflections. ‡ R factor = $\sum_{hkl} ||F_{obs}| - |F_{calc}|| / \sum_{hkl} |F_{obs}|$, where F_{obs} and F_{calc} are the observed and calculated structure-factor amplitudes, respectively. § R_{free} was calculated with 5% of the data excluded from the refinement. ¶ Root-mean-square deviation from ideal values. †† Categories were defined by *MolProbity*.

2.4. Structure determination and refinement

The structure was determined by molecular replacement with the program *MOLREP* (Vagin & Teplyakov, 1997) from the *CCP*4 suite (Collaborative Computational Project, Number 4, 1994) using the structure of GABA-A receptor-associated protein (GABARAP; PDB code 1kjt; Bavro *et al.*, 2001) as a search model. The initial model was refined by using the maximum-likelihood method and TLS refinement to refine the anisotropic *B* factors as implemented in *REFMAC*5 (Murshudov *et al.*, 1997) as part of the *CCP*4 program suite and was rebuilt interactively using σ_A-weighted electron-density maps with coefficients $2mF_o - Fc$ and $mF_o - Fc$ in the program *Coot* (Emsley & Cowtan, 2004). The final model was validated with the programs *PROCHECK* (Laskowski *et al.*, 1993) and *MolProbity* (Chen *et al.*, 2010). Structure factors and coordinates have been deposited in the Protein Data Bank (PDB; http://www.rcsb.org/pdb) under accession code 3m95.

3. Results and discussion

3.1. Overall structure

The crystal structure of BmAtg8 was refined to a resolution of 2.40 Å. There are two subunits (*A* and *B*) in the asymmetric unit, but the symmetry relating them was not imposed during refinement. The majority of residues are fitted well in the electron-density map, except for the N-terminal His tag of both subunits. Statistics of the X-ray data-collection and refinement statistics are summarized in Table 1.

The overall structure of BmAtg8 consists of a four-stranded β-sheet (β1–β4) flanked by two pairs of α-helices (α1–α2 and α3–α4),

one on each side of the sheet (Fig. 1). The core domain, a ubiquitin fold, consists of four β-strands (β1–β4) with two of the α-helices (α3–α4) on one side of the sheet. In BmAtg8, two additional α-helices (α1 and α2) cover the other side of the sheet *via* both polar and hydrophobic interactions.

3.2. Structure comparison

Several crystal structures of Atg8 homologues have been reported. Multiple sequence alignment indicates that Atg8 is highly conserved from yeast to mammals (Fig. 2*a*). We found that BmAtg8 shows high structural similarity to the search model GABARAP (PDB code 1kjt; Bavro *et al.*, 2001), microtubule-associated protein light chain 3 (LC3; PDB code 1ugm; Sugawara *et al.*, 2004), *Trypanosoma brucei* Atg8 (TbAtg8; PDB code 3h9d; Koopmann *et al.*, 2009) and *S. cerevisiae* Atg8 (ScAtg8; PDB code 2zpn; Noda *et al.*, 2008), with root-mean-square deviations (r.m.s.d.s) of 0.5, 0.9, 1.1 and 0.8 Å over 110 C^{α} atoms, respectively (Fig. 2*b*). The helices α1 and α2 sustain their orientation *via* tight interactions with the ubiquitin core by means of several hydrogen bonds and salt bridges. In detail, residues Phe3, Gln4, Tyr5, Lys6, Ile21, Arg22, Tyr25, Arg28 and Glu34 contribute to the hydrogen bonding. Four salt bridges were found: between Lys6 and Asp100, between Arg14 and Asp102, between Lys15 and Glu101 and between Glu17 and Lys48 (Fig. 3). Most of these residues are highly conserved from yeast to mammals. This implies that these conserved residues are essential for the protein to maintain its structural integrity and biological function (Sugawara *et al.*, 2004). In BmAtg8, residues His9 and Ser10 on the loop between α1 and α2 also contribute to the stabilization of the N-terminal helices. His9 can form hydrogen bonds to Tyr5 and Arg14. Ser10, which is not conserved in the homologues, forms hydrogen bonds to Lys13 and Arg14.

Two hydrophobic pockets are found to exist in all Atg8 homologues. One pocket comprises Glu17, Ile21, Pro30, Ile32, Lys48 and Leu50 and is located between helix α2 and the core domain and the other comprises Tyr49, Val51, Pro52, Phe60, Leu63 and Ile64 and is located in the ubiquitin fold. Most residues in the hydrophobic

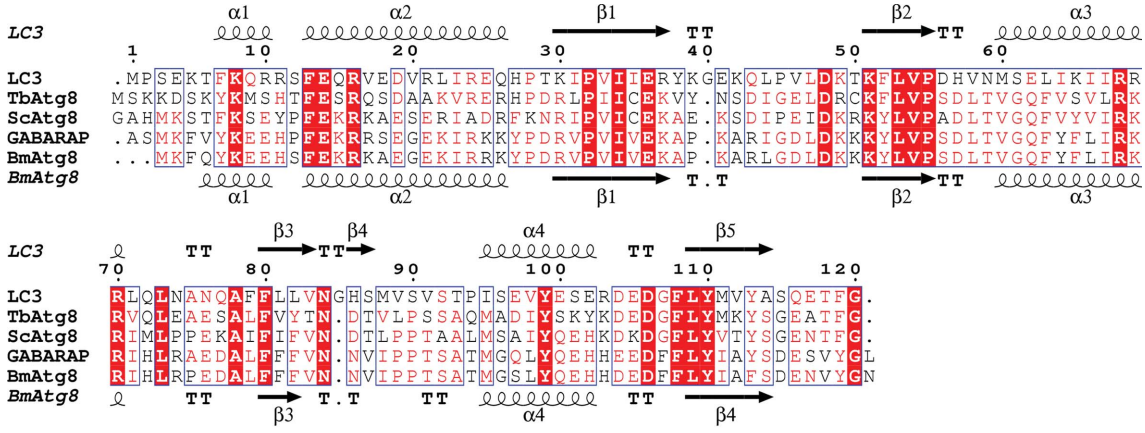

(*a*)

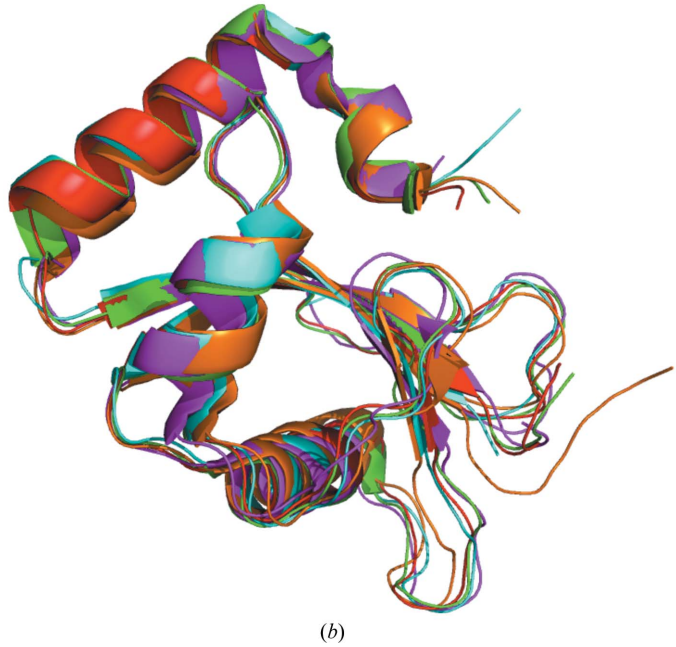

(*b*)

Figure 2
Structure comparison. (*a*) Structure-based sequence alignment of microtubule-associated protein light chain 3 (LC3; 33% identity), *T. brucei* Atg8 (TbAtg8; 46% identity), *S. cerevisiae* Atg8 (ScAtg8; 56% identity) and GABARAP (90% identity) with BmAtg8. The sequences of homologues of BmAtg8 were obtained from the PDB. The secondary structure of LC3 is shown at the top and that of BmAtg8 is shown at the bottom. Alignments were performed using the programs *MULTALIN* (Corpet, 1988) and *ESPript* (Gouet *et al.*, 2003). Conserved residues are marked by blue boxes and identical residues are shown in red. (*b*) Overall structure superposition of BmAtg8 (red) with GABARAP (green), LC3 (magenta), TbAtg8 (orange) and ScAtg8 (cyans). This figure was prepared using *PyMOL* (DeLano, 2002).

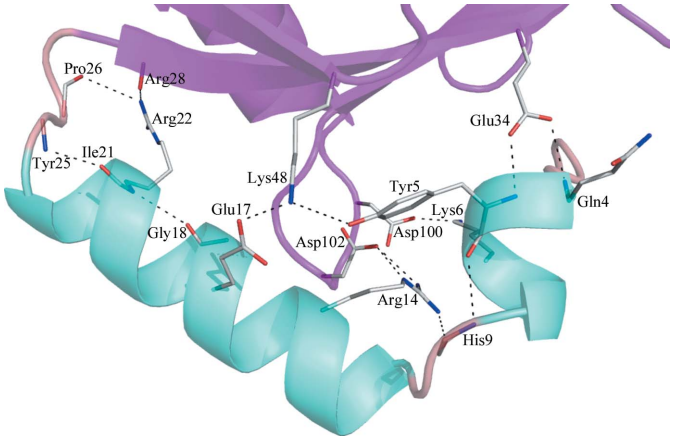

Figure 3
Interactions between the ubiquitin fold and the N-terminal helices. The N-terminal helices are coloured cyan and the ubiquitin fold is coloured magenta. The residues contributing to the interactions are labelled. This figure was prepared using *PyMOL* (DeLano, 2002).

pockets are also conserved in different species. As reported previously (Noda *et al.*, 2008), these pockets are involved in the interaction between LC3 and p62: the side chains of residues Trp338 and Leu341 in p62 insert deeply into these pockets and an intermolecular β-sheet is formed by p62 and β2 in LC3. This suggests that these regions in BmAtg8 are potential binding sites that recognize other protein partners in a similar manner.

In conclusion, BmAtg8 contains a ubiquitin fold which has been found in all Atg8 proteins from yeast to mammals. The high conservation in the structure of Atg8 illustrates that the Atg8 protein plays a central role in the autophagy pathway of eukaryotes.

This work was sponsored by the Chinese National Natural Science Foundation (grant 90608027), the Hi-Tech Research and Development Program of China (grant 2006AA10A119), the 973 project (grant 2005CB121002) from the Ministry of Science and Technology of China and the Knowledge Innovation Program of the Chinese Academy of Science.

References

Amar, N., Lustig, G., Ichimura, Y., Ohsumi, Y. & Elazar, Z. (2006). *EMBO Rep.* **7**, 635–642.
Bavro, V. N., Sola, M., Bracher, A., Kneussel, M., Betz, H. & Weissenhorn, W. (2001). *EMBO Rep.* **3**, 183–189.
Chen, V. B., Arendall, W. B., Headd, J. J., Keedy, D. A., Immormino, R. M., Kapral, G. J., Murray, L. W., Richardson, J. S. & Richardson, D. C. (2010). *Acta Cryst.* D**66**, 12–21.
Collaborative Computational Project, Number 4 (1994). *Acta Cryst.* D**50**, 760–763.
Corpet, F. (1988). *Nucleic Acids Res.* **16**, 10881–10890.
Cuervo, A. M. (2004). *Trends Cell Biol.* **14**, 70–77.
DeLano, W. L. (2002). *The PyMOL Molecular Viewer.* DeLano Scientific LLC, San Carlos, California, USA. http://www.pymol.org.
Emsley, P. & Cowtan, K. (2004). *Acta Cryst.* D**60**, 2126–2132.
Gouet, P., Robert, X. & Courcelle, E. (2003). *Nucleic Acids Res.* **31**, 3320–3323.
Ichimura, Y., Kirisako, T. & Takao, T. (2000). *Nature (London)*, **408**, 489–493.
Klionsky, D. J., Cregg, J. M., Dunn, W. A. Jr, Emr, S. D., Sakai, Y., Sandoval, I. V., Sibirny, A., Subramani, S., Thumm, M., Veenhuis, M. & Ohsumi, Y. (2003). *Dev. Cell*, **5**, 539–545.
Koopmann, R., Muhammad, K., Perbandt, M., Betzel, C. & Duszenko, M. (2009). *Autophagy*, **5**, 1085–1091.
Laskowski, R. A., MacArthur, M. W., Moss, D. S. & Thornton, J. M. (1993). *J. Appl. Cryst.* **26**, 283–291.
Murshudov, G. N., Vagin, A. A. & Dodson, E. J. (1997). *Acta Cryst.* D**53**, 240–255.
Nakatogawa, H., Ichimura, Y. & Ohsumi, Y. (2007). *Cell*, **130**, 165–178.
Noda, N. N., Kumeta, H., Nakatogawa, H., Satoo, K., Adachi, W., Ishii, J., Fujioka, Y., Ohsumi, Y. & Inagaki, F. (2008). *Genes Cells*, **13**, 1211–1218.
Reggiori, F. & Klionsky, D. J. (2002). *Eukaryot. Cell*, **1**, 11–21.
Shintani, T. & Klionsky, D. J. (2004). *Science*, **306**, 990–995.
Sugawara, K., Suzuki, N., Fujioka, Y., Mizushima, N., Ohsumi, Y. & Inagaki, F. (2004). *Genes Cells*, **9**, 611–618.
Vagin, A. & Teplyakov, A. (1997). *J. Appl. Cryst.* **30**, 1022–1025.
Xie, Z., Nair, U. & Klionsky, D. J. (2008). *Mol. Biol. Cell*, **19**, 3290–3298.
Zhang, X., Hu, Z.-Y., Li, W.-F., Li, Q.-R., Deng, X.-J., Yang, W.-Y., Cao, Y. & Zhou, C.-Z. (2009). *BMC Mol. Biol.* **10**, 50.